Quantum Design

Application Note 1084-306

Measurement of Electrical Resistivity Without Contacts Using the ACMS Option

by N. R. Dilley and M. Baenitz

[This is a new revision of an application note by L. Brinker and M. Baenitz (then at Freie Universität Berlin) that was originally published in issue 7 of the Quantum States newsletter (1998)]

Introduction

Attaching transport leads to a sample in order to measure its electrical resistance can be difficult or impractical if the sample is, say, air-sensitive, liquid or has an insulating barrier on the surface. However, it is possible to deduce the resistivity of a regularly shaped sample from its response to an a.c. magnetic field, a technique that does not require any connections be made to the sample. The electrical resistivity of a sample can be deduced from a change in mutual inductance between two coils when the sample is inserted into them. This has been described by a number of authors. For substances which are nonmagnetic or very weakly magnetic this leads to a decrease in the mutual inductance M between the coils. A weakly magnetic material is one in which the magnetic permeability $\mu \approx 1$ (NOTE: we will use cgs units in this application note unless stated otherwise). Thus, we will be neglecting intrinsic magnetic properties of the sample in this discussion, whether the sample is paramagnetic (μ>1) or diamagnetic (μ<1) and will instead be focusing only on the inductive properties of electrically conductive samples. The reduction in mutual inductance dM can be expressed in the form $dM = dM' + idM''$ wherein the imaginary part dM'' is derived from losses due to induced eddy currents. By measuring dM' and dM'' or, in our case, the real and imaginary parts of the a.c. magnetic moment m' and m'', the sample's specific resistivity can be determined. Note that $m' = \chi' \cdot H_{ac}$ where χ' is the real part of the a.c. susceptibility and H_{ac} is the applied a.c. magnetic field. Concerning systematic errors, the inductive method is potentially better as it requires only the knowledge of the sample radius r while the standard bulk transport method requires measurement of the sample cross-section as well as the separation of the voltage leads.

Theory

Starting from the Maxwell equations for an alternating field in cylindrical coordinates:

$$\vec{H}(r,\varphi,t) = \vec{H}(r,\varphi) \cdot e^{-i\omega t} \qquad (1)$$

inside a material of isotropic resistivity, the response satisfies the equation:

$$\nabla^2 \vec{H} = -\frac{4\pi i \mu\omega}{c^2 \rho}\vec{H} = -\frac{2i}{\delta^2}\vec{H} \tag{2}$$

where c is the speed of light, ρ is the sample resistivity and δ is the skin depth of the material (in cgs units):

$$\delta = \frac{c}{2\pi}\sqrt{\frac{\rho}{\mu f}} \tag{3}$$

and $f = \omega / (2\pi)$ is the frequency in Hz. For ease of calculation, we also write the skin depth equation in which the sample resistivity ρ is expressed in μΩ-cm:

$$\delta = 5.04\sqrt{\frac{\rho[\mu\Omega - cm]}{\mu f[Hz]}} \tag{4}$$

Note that the theory here works only if the permeability is close to unity and is not complex (as is the case near a magnetic phase transition).

Solving this differential equation for a cylindrical sample whose axis is parallel to the magnetic field (see ref. III for more details) and expressing in terms of the dimensionless a.c. susceptibility yields:

$$\chi = \chi' + i\chi'' = -\frac{1}{4\pi}\frac{J_2\left(\xi \cdot i^{1/2}\right)}{J_0\left(\xi \cdot i^{1/2}\right)} \tag{5}$$

J_2 and J_0 are Bessel functions of the first kind, and:

$$\xi = \sqrt{2}\frac{r}{\delta} = \frac{\pi r}{c}\sqrt{\frac{8f}{\rho}} \tag{6}$$

where r is the radius of the cylindrical sample. Note that:

$$\chi' = \frac{m'}{H_{ac}V} \tag{7}$$

(and similarly for the χ'') where m' is the measured in-phase moment (in emu) and V is the sample volume (in cm^3). The problem is one of deducing ξ and hence ρ from the measured quantities m' and m'' .

Shown in Figure 1 is a graph of $4\pi\chi$ of a nonmagnetic conducting sample versus the argument ξ (data for the plot is taken from ref. III).

We found ref. III to be a very good resource in general – keep in mind that the notation in that paper is subtly different: the quantity m' is a dimensionless ratio of mutual inductance (not the a.c. moment) and ξ is written there as x.

For better visualization in terms of measured quantities, we also include Figure 2 which expresses the a.c. susceptibility as a function of a.c. frequency for the material properties of a 2 mm radius copper cylinder at 300 K.

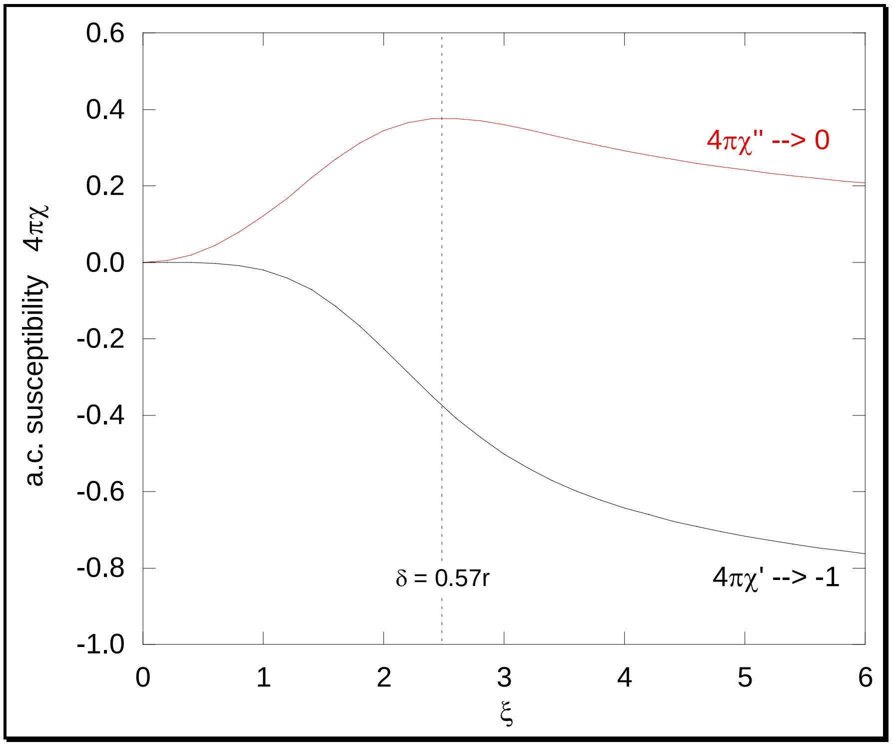

Figure 1: a.c. susceptibility of a long cylindrical sample with axis parallel to the magnetic field

Referring to Figure 1, the peak in χ'' occurs when the skin depth is about half the cylinder radius. This peak can cause issues with some analysis methods as the χ'' vs. ξ plot is not single-valued. This problem is averted if one maps the a.c. response in terms of the phase shift due to the sample (recorded in the ACMS measurement .DAT file as "Phase(deg)"):

$$\Delta\phi = \arctan\left(\frac{m''}{m'}\right) \tag{8}$$

Using the tabulated values from ref. III for m' and m'' (the ratio will be the same whether *m* refers to inductance ratio or magnetic moment), Figure 3 is generated.

One can model the curve to obtain a numerical conversion between $\Delta\phi$ and ξ and thus deduce the resistivity at any given frequency. More details about our specific methods to that end are given in the next section.

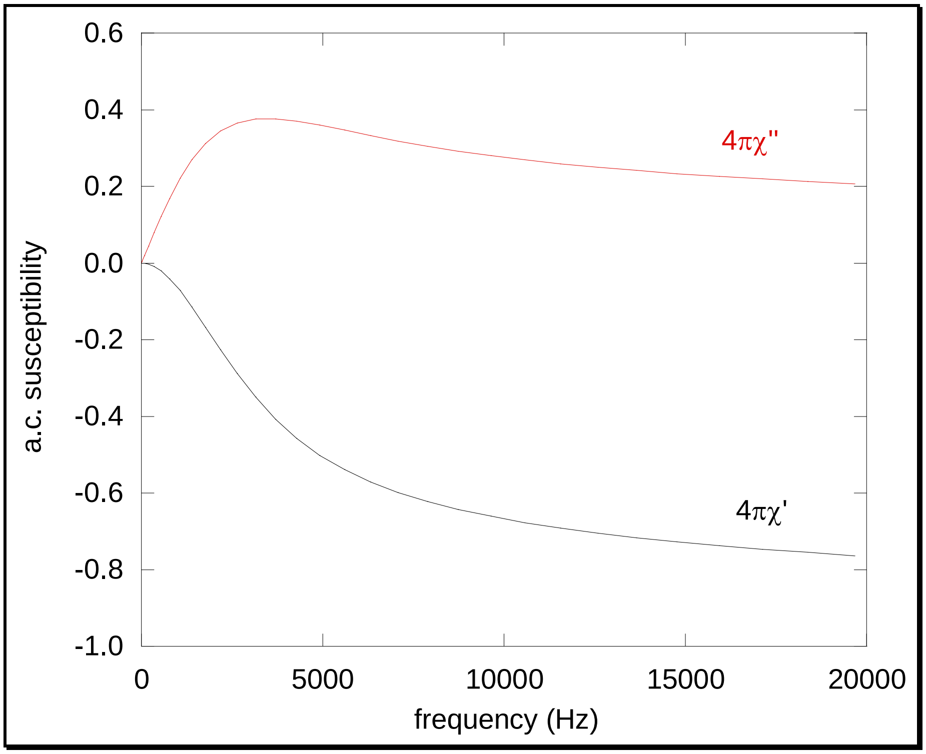

Figure 2: theoretical response of a 2 mm radius Cu cylinder at 300 K (ρ=1.72 μΩ-cm)

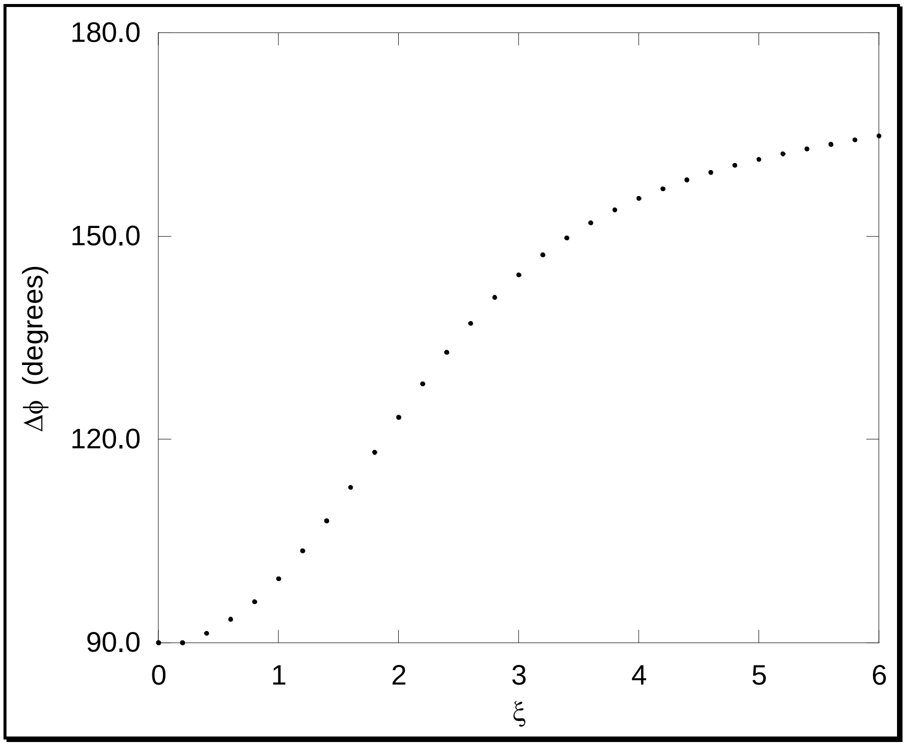

Figure 3: a.c. measurement phase shift is a single-valued function of ξ

Figure 4 is included as a heuristic tool to show the influence of sample magnetism on the measured a.c. susceptibility. In addition to the induced eddy currents in the conductor, there is a contribution to χ' from the magnetic polarization of the sample in the a.c. field: Pauli paramagnetism of the conduction electrons, Landau diamagnetism, Larmor diamagnetism (of core-level electrons), Curie-Weiss paramagnetism of local spins, and so on. This can be seen clearly if measuring the Pd standard sample included with the ACMS option: at low frequencies one sees a positive and frequency independent χ' due to the large paramagnetic moment of Pd but at higher frequencies the eddy current screening dominates and a negative χ' is observed. In addition, the eddy currents screen the field from the inside of the sample so the magnetic response of the sample is further attenuated as can be seen in the plot below as the three curves converge toward high values of ξ. Thus, if one is using an analysis technique that involves χ' (such as the $\Delta\phi$ method), the sample magnetism contribution to χ' must be removed before proceeding. This is usually achievable by using sufficiently high frequencies such that $\delta < r$.

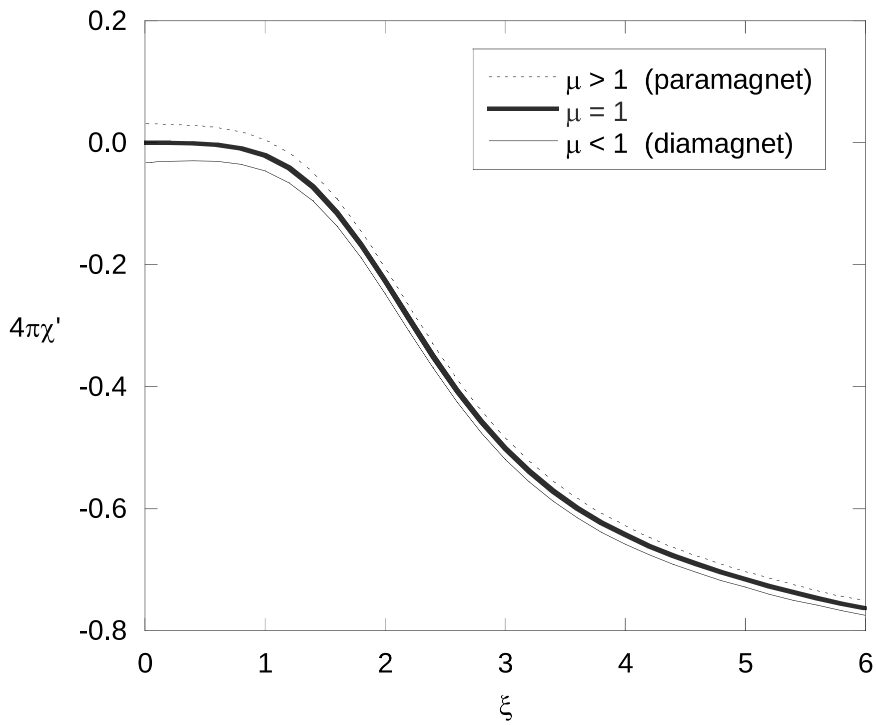

Figure 4: influence of paramagnetism and diamagetism on in-phase a.c. response

Based on the above discussion, we can place the following requirements on a sample in order to make a successful contactless resistivity measurement using the ACMS option of the PPMS:

- sample can be shaped into a cylinder that is:
    - long in order to avoid sample end effects (12 mm high samples were measured here)
    - large enough diameter to generate eddy currents: this is due to the quadratic dependence of χ'' on r for small values of r/δ
- sample resistivity is isotropic
- sample resistivity is in the range of typical metals (0.01 – 100 μΩ-cm)
- sample magnetism is weak compared to the inductive response and/or can be suitably subtracted (see Figure 4), otherwise there will be a systematic error in $\Delta\phi$

Data Acquisition

Some authors (ref. II) tried to solve the problem of solving the Bessel functions by building their devices so that the response signal in the secondary coil is directly proportional to the resistivity of the material. This only works properly for one particular frequency since stray capacitances, etc. could cause unreliable data. Among the several analysis methods described by Chambers and Park (ref. III), one was to use polynomial approximations for the Bessel functions which are valid either for large or small values of ξ. This implies that the sample's resistivity must be approximately known in advance of performing the analysis.

In order to determine the resistivity of a variety of samples in a wide range of frequencies, we wrote a program in Turbo Pascal which calculates the Bessel functions using an algorithm from ref. (IV) for a fixed starting value ξ_{start} and then using equation (8) to calculate the corresponding value $\Delta\phi'_{start}$. After this, the program changes the ξ-value until the difference between the calculated value $\Delta\phi'$ and the measured phase shift $\Delta\phi$ is less than 1 ppm. Each calculation took less than 40 steps per measured data point.

To test the measured data for errors which might be derived from an artificial phase offset of -90 deg occurring with very weak signals (total moment < 10^{-6} emu), the above calculation should be repeated at a few different frequencies.

Experiment

The cylindrical shaped samples were inserted parallel to the axis of the alternating magnetic field. To avoid end-effect errors (which are not considered in the theory described above) we used samples with a length of approximately 12 mm and a radius of between 0.5 and 2.5 mm. While measuring the amplitude and phase of the a.c. magnetization, we applied an a.c. magnetic field of not less than 10 Oe since the response signal becomes more stable when the field is higher. The frequency of the applied field ranged from 1 kHz to 10 kHz. As a general rule, it is best to keep the frequency near the peak in $\chi''(\xi)$ (see Figure 1) so that the slope of $\Delta\phi$ vs. ξ is highest (see Figure 3) and thus the systematic errors in the derivation of ξ are lowest. For poor conductors such as indium, higher frequencies are advantageous in order to achieve stable phase signals. The measured data for the a.c. magnetization over a wide range of temperatures were later exported and written into our program for resistivity calculations.

Figure 5 shows our calculated values for measurements of oxygen-free copper (left) and gold (right) in comparison with values from literature (ref. V). In the case of copper we also performed a direct resistance measurement by applying the 4-probe method (using the bridge board of our PPMS). The difference between literature and measured values for the low temperature part of the resistivity of copper is derived from impurities in our sample.

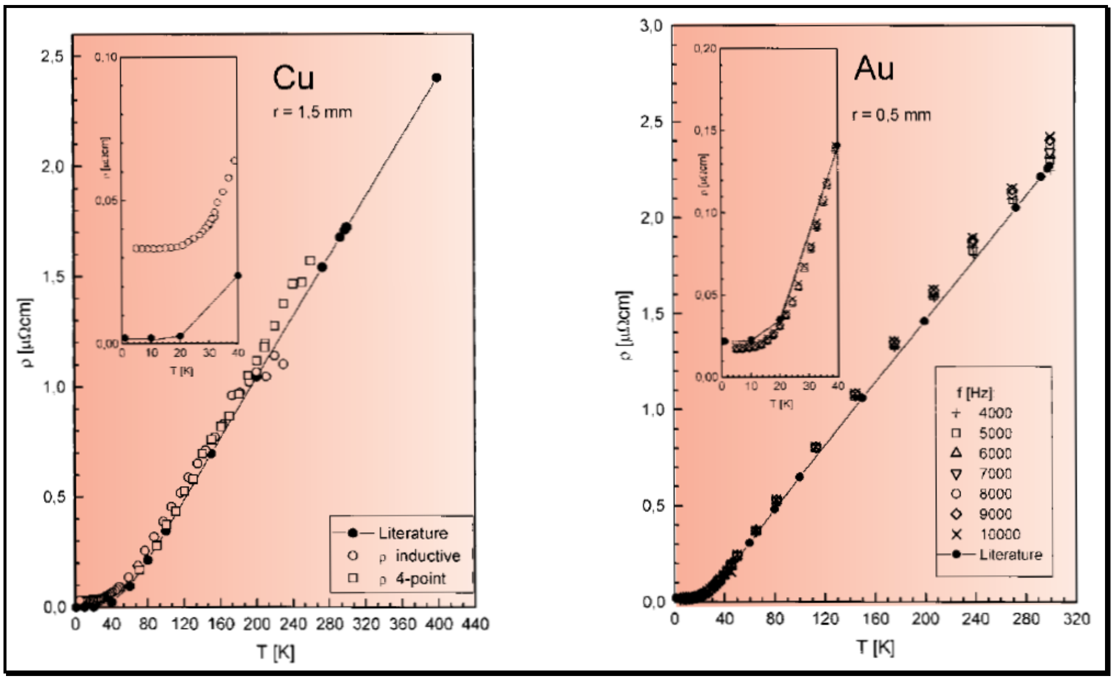

Figure 5: (LEFT) resistivity of oxygen-free copper determined with the inductive method (open circles) and those determined from the 4-point method (open squares) in comparison with data from literature (ref. V). (RIGHT) Resistivity of gold plotted versus temperature. The full circles are derived from literature (ref. V). Other symbols are calculated values from inductive measurements with different frequencies of the applied a.c. magnetic field.

A very interesting result is shown in Figure 6. Here we measured a pressed powder sample of the superconductive material Nb_3Sn (Tc ≈ 18 K). The graph shows the calculated resistivity from inductive measurements in comparison with those of the direct 4-point method. The difference between the absolute values is a surprising factor of 20, whereas the temperature dependence in both measurements is identical.

We interpret this difference in absolute values as a result of non-homogeneous potential distributions within the powder specimen where the 4-point method is applied. In order to get the sample resistivity values, one should use an effective cross section and length of the specimen.

Acknowledgements
The investigation of this method was performed in the research group of Prof. K. Lüders, Fachbereich Physik, Freie Universität Berlin, Germany and supported by the Bundesministerium für Bildung, Wissenschaft, Forschung und Technologie (BMBF Nr. 13 N 6660/3). The authors are obliged to Prof. Lüders and the members of his group for helpful discussions and to R. Pues who started the investigation of the contactless resistivity method. ND acknowledges valuable insights, contributions and corrections to the original application note that were offered by John McCloy, Tim Droubay and Jaehun Chun of Pacific Northwest National Laboratory.

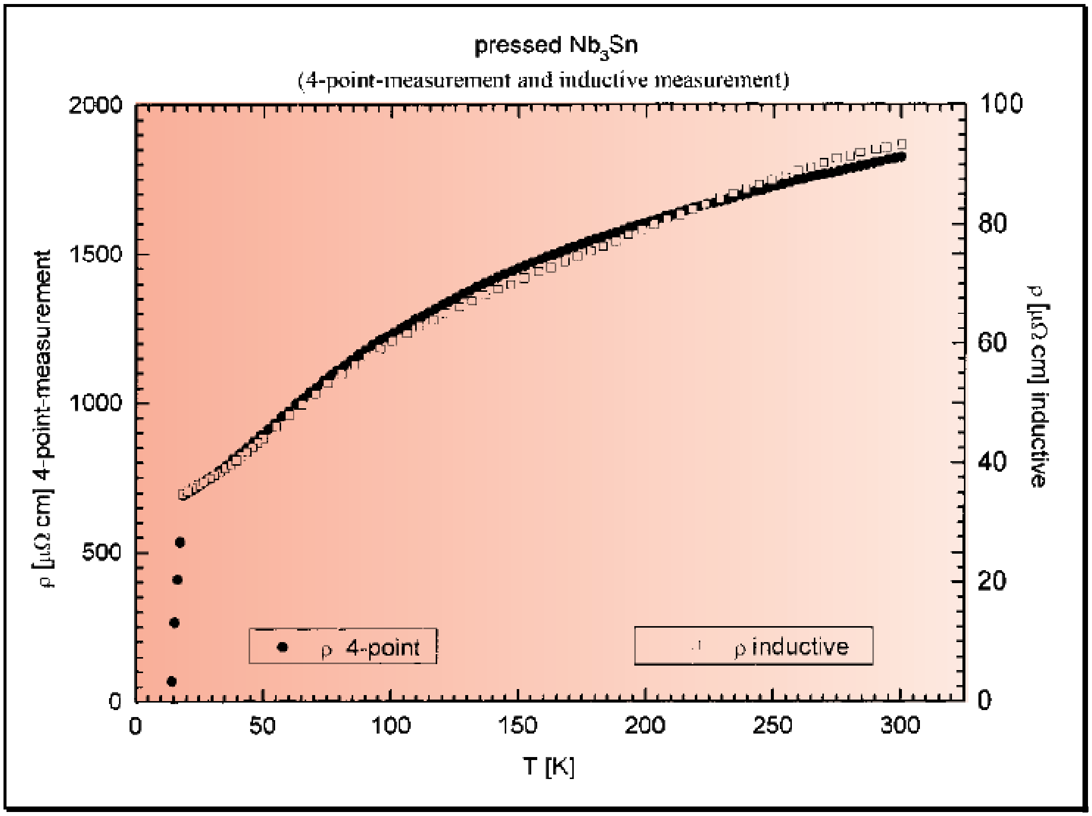

Figure 6: Calculated resistivity deduced with the inductive method (right axis, open squares) and the 4-point transport method (left axis, full circles).

References

[I] L. D. Landau, E. M . Lifshitz and L.P. Pitaevskii, *Electrodynamics of Continuous Media*, 2nd edition, Pergamon Press, 1984.

[II] Ya. A. Kraftmakher, *Meas. Sci Technol*. **2** (253) 1991.

[III] R. G. Chambers, J. G. Park, *British Journal of Applied Physics* **12** (507) 1961.

[IV] W. H. Press, B. P. Flannery, A. A. Teukolsky, W. T. Vetterling, *Numerical Recipes in C*, 2nd edition, Cambridge University Press, 1992.

[V] *CRC Handbook of Chemistry and Physics*, 84th edition, CRC Press London, 2003.